CALSPAN ADVANCED TECHNOLOGY CENTER

31 August 1978

ANOTHER STUDY OF THE T-38A PIO INCIDENT

Prepared by: C. R. Chalk

C. R. Chalk
Staff Engineer

CRC/jc

A DIVISION OF CALSPAN CORPORATION
AN ARVIN COMPANY P.O. BOX 400 BUFFALO, NEW YORK 14225

ANOTHER STUDY OF THE T-38A PIO INCIDENT

INTRODUCTION

The T-38A aircraft as configured in the early 1960 versions was PIO prone at low altitude and high speed. A specific PIO incident was recorded during a flight of an instrumented airplane in 1960. Time histories of several parameters recorded during that incident have been published in various reports, References 1, 2, 3, and 4. These time histories are reproduced as Figure 1 in this memo. The T-38A PIO problem was studied by an Air Force review board in Reference 1, by Northrop in Reference 2, and by STI in Reference 3 during the time in 1963-64 when a fix for the airplane was being developed. The T-38A PIO incident has also been used as an example by other authors in attempts to develop theoretical explanations for that PIO incident and in attempts to develop requirements for incorporation in the flying qualities specification. Examples are the work by Neal in Reference 5 and Smith in Reference 4.

While reviewing the work reported by Smith in Reference 4, the author of this paper became interested in attempting to model the pilot's contribution to the dynamic system that would be required to cause the dynamic instability exhibited in the time histories of Figure 1. This paper documents the results of the study performed.

THE T-38A PIO TIME HISTORY

The following observations are drawn from study of the time histories of Figure 1.

1. At the beginning of the record, the flight control system is in a limit cycle oscillation with a frequency of $\omega = 22.2$ rad/sec. The pilot is not applying any force to the control stick.

2. At 7.7 sec on the time scale, the pilot switched the pitch damper OFF. This action interrupted the limit cycle with the stabilizer at one extreme of the oscillation. This trailing-edge-up stabilizer deflection caused the airplane to pitch up and pull 3 g.

3. During the first 0.3 sec after the pilot switched the pitch damper OFF, the pilot did not apply any stick force, but the stabilizer moved toward trim. This stabilizer motion could be a result of the action of the bobweight or it might be a result of the pitch damper actuator going through a "center and lock action".

4. At approximately 0.3 sec after the pilot switched the damper OFF, he applied a sharp push force to the stick to stop the pitch-up. At approximately t = 8.4 sec, the stick force is reversed briefly and for the next 5 seconds, the pilot-control system-airplane combination is involved in a violent PIO oscillation that is neutrally stable to slightly unstable. During this time, the mean pitch attitude is approximately 15^{o} nose up.

5. During the period $13 < t < 16$ sec, the pilot applied an average push force which caused the airplane to pitch over to approximately 7^{o} nose-up attitude.

6. During the period $16 < t < 21$ sec, the record exhibits a continuing oscillation of approximately 1/5 the previous amplitude.

7. The frequency of the PIO is approximately $\omega = 7.4$ rad/sec. This oscillation is exhibited in all of the recorded parameters. The stick force time history exhibits a higher frequency oscillation, $\omega \cong 19.6$ rad/sec, that is associated

with the control system. This oscillation is also very lightly damped.

8. The frequency and damping ratio of the oscillatory modes can be fairly accurately estimated from the time histories but relative phase information and amplitude information must be viewed with caution becuase the filtering of the sensors and recording channels is not known. Also, the pitch rate and normal acceleration traces are somewhat distorted sine waves which might indicate a structural mode is involved. The accelerometer trace is very smooth and exhibits no high frequency modes or "hash" typical of accelerometers. This could be the result of eyeball fairing the time history while hand tracing it for presentation in a report. The peaks of the $\dot{\theta}$ trace lag the maximum slopes of the θ trace by approximately 0.10 sec or 41° at the PIO frequency. The stick force trace also exhibits a phase relative to the pitch attitude trace that is inconsistent with the transfer functions listed in Reference 6 for the control system, surface actuator and airplane. Evaluation of the θ/F_s transfer function at $\omega = 7.4$ rad/sec gives

$$\theta/F_s = .404\ e^{-74.49^{\circ}j} \quad \text{deg/lb}$$

whereas estimation from the time histories indicates

$$\theta/F_s = .55\ e^{-255^{\circ}j} \quad \text{deg/lb}$$

Figure 2 illustrates the θ and F_s time histories and phase relation at $\omega = 7.4$ rad/sec. This discrepancy between the calculated and measured values could be caused by the transfer functions not representing the airplane and control system. Since the phase shift is nearly 180°, it suggests that possibly the push and pull labels on the F_s time history

may be reversed. Examination of the initial pilot input and its effect in stopping the pitch up and also the fact that the average push force applied from t = 13 to t = 16 sec did result in a nose-down airplane response establishes that the recording senses and the trace motions are consistent for low frequency. The values of the transfer function parameters used to calculate the amplitude ratio and phase angle at ω = 7.4 rad/sec were taken from Reference 6 which is bound as a section in Reference 1. The data used by STI was obtained from Northrop and Northrop derived the data from analysis, wind tunnel data, ground test of the control system and flight test on the T-38A family of aircraft. T-38A SN 59-1602 was the test aircraft used to develop fixes for the PIO problem. The PIO record illustrated in Figure 1 was taken in a different aircraft, SN 58-1194.

The large difference between the calculated and measured values of the phase of the θ response to F_s at ω = 7.4 rad/sec is of concern and must be kept in mind as a tempering factor in interpreting any analysis based on use of the transfer functions of Reference 6 to describe the T-38A dynamic characteristics. The stick-free transfer functions were developed by STI using pitch attitude to stabilizer deflection transfer function and stabilizer deflection to stick force transfer function data and calculation of the effect of normal acceleration at the bobweight fed back through the bobweight system. This analysis did not account for fore and aft acceleration effects on the control system or for angular acceleration effects on the control system components with significant rotary inertia.

9. Neither the stablizer nor the stick force trace exhibit any discontinuities that would indicate significant control system friction effects.

ROOT LOCUS ANALYSIS

The following assumptions were made as a basis for performing a root locus analysis of the T-38A PIO.

1. It was assumed that the transfer functions developed in Reference 6 represent the stick free T-38A with the bobweight active. See Table 1.

2. It was assumed that the system was linear. No account was taken of friction, etc.

3. It was assumed that the pilot-control system-airplane dynamic system during the PIO of Figure 1 is exhibiting two neutrally stable roots with frequencies

$$\omega_L = 7.4 \text{ rad/sec}$$

$$\omega_H = 19.6 \text{ rad/sec}$$

4. Because the stability of the high frequency flight control system mode is of interest and pilot transfer functions with transport delay are to be assumed, it was decided to use the exact representation of the transport delay developed in Reference 7 rather than the Pade approximation.

The T-38A PIO has been analyzed in Reference 3 and 4 using the following pilot transfer functions for pitch attitude loop closure and separately for loop closure of normal acceleration at the pilot station.

"Equalized" Pilot $\quad Y_{p_\theta} = \dfrac{K_\theta e^{-.2s}}{\left[\frac{s}{3.2} + 1\right]}$, $Y_{p_{n_z}} = \dfrac{K_{n_z} e^{-.2s}}{\left[\frac{s}{3.2} + 1\right]}$

"Primitive" Pilot $\quad Y_{p_\theta} = K_\theta e^{-.2s}$, $Y_{p_{n_z}} = K_n e^{-.2s}$

Root locus diagrams illustrating the effect on the closed loop system roots for each of these pilot transfer functions are contained in Figures 3, 4, 5 and 6. None of these root loci result in roots becoming unstable at the frequencies observed in the PIO time history, i.e., ω = 7.4 and ω = 19.6 rad/sec. Also none of these loci show two roots becoming unstable simultaneously at these two frequencies.

Many feedback parameters and forms for the pilot transfer function were assumed and root locus plots were calculated in attempts to force the short period and control system roots to become neutrally stable at ω = 7.4 and ω = 19.6 rad/sec for the same gain value. No solution was found for single variable feedback. Multiple solutions were found, however, when feedback of three airplane responses was used, e.g., θ, $\dot{\theta}$ and $\ddot{\theta}$ or n_z, θ and $\dot{\theta}$ with a time delay included in the pilot model.

The four pilot transfer functions listed in Table 2 will all cause the system root locus branches to pass into the right half plane at ω = 7.4 and ω = 19.6 for a given value of loop gain in each case. The root locus diagrams are shown in Figures 7-10.

Although these pilot model transfer functions are impressively complicated and the root locus diagrams are intricate and computer plotted, they are, in fact, meaningless because they are based on an invalid model of the T-38A airplane and control system. Once this fact was realized, the author set about trying to identify a more valid mathematical model of the T-38A and in the process "discovered" that the primary cause of the T-38A PIO phenomena was the horizontal stabilizer servo actuator control valve. The evidence available in the published reports that leads to this conclusion is presented and discussed below.

The discrepancy in phase angle of pitch attitude relative to stick force in the PIO record of Figure 1 relative to the phase angle calculated from the analytical model was noted previously and is illustrated in Figure 2. The two phase angles are different by 181°, In order to evaluate the

source of this discrepancy, a photo enlargement was made of Figure 1 and onion skin tracings were made of the traces. The traces could then be shifted and overlayed to establish fairly accurately their relative phase angles. The results of this analysis are shown in Figure 11 in the form of a phaser diagram using stick force as the reference. This figure illustrates the large difference in $\theta - F_s$ phase from the PIO record compared to the analytical model. It also illustrates a 41^o lag of pitch rate measured from the PIO record relative to a 90^o phase advance from the θ reference. This lag is probable due to a structural mode. This conclusion is supported by the shape of the $\dot{\theta}$ time history in Figure 12 (damper OFF). The $n_{\frac{\dot{\theta}}{\delta}}$ phaser in Figure 11 indicates some lag from the analytical phase lead from $\dot{\theta}$ that was calculated from the ratio of transfer function numerators. This lag might also be due to the structural mode or perhaps partly from recording filtering. The stabilizer time history in the PIO record goes off paper before the PIO sine wave becomes established and therefore its phase at the PIO frequency could not be estimated from the PIO record. The stabilizer phase relative to the pitch attitude phaser can be estimated from the stick fixed θ/δ_H transfer function, however, so effort was spent in searching out data to establish the stick-fixed and stick-free short period dynamics. The data in References 1, 2, 6, and 9 are plotted in Figure 13. The calculated values for stick-fixed and stick-free short period do not agree with the measured data. It seems apparent that the stick-free short period calculated in Reference 6 by assuming a simple $n_{\frac{\dot{\theta}}{\delta}}$ bobweight effect was not an adequate model. The stick-fixed data displayed in Figure 13 for doublet responses indicate the following short period roots:

$$\text{Stick Fixed} \quad \omega_{n_{sp}} = 7.0 \text{ rad/sec} \quad \zeta_{sp} = .4$$

The stick-free short period dynamics are less precisely defined by the data in Figure 13. The data indicate a stick-free model roughly as follows:

$$\text{Stick Free} \quad \omega'_{n_{sp}} = 7.0 \quad \zeta'_{sp} = .14$$

which is significantly different from the model in Table 1.

The stick-fixed θ/δ_H transfer function was evaluated at $\omega = 7.4$ which gave a phase lag of 128°. This angle was used to locate the δ_H phaser relative to the θ phaser in Figure 11 for the PIO record set. These calculations suggest that the analytical model of the feel system and servo actuator δ_H/F_s is wrong by approximately 174°. In Reference 5 the following stick-free transfer function for the T-38A control system is derived:

$$\frac{\delta_H}{F_s} = \frac{K\left[\frac{s^2}{\omega_{n_{sp}}^2} + \frac{2\zeta_{sp}}{\omega_{n_{sp}}} s + 1\right]}{\left(\frac{s}{\tau_s'} + 1\right)\left[\frac{s^2}{\omega_{n_{F_s}}'^2} + \frac{2\zeta_{F_s}'}{\omega_{n_{F_s}}'} s + 1\right]\left[\frac{s^2}{\omega_{n_{sp}}'^2} + \frac{2\zeta_{sp}'}{\omega_{n_{sp}}'} s + 1\right]}$$

The phase contributions of each of the factors of this transfer function are noted on Figure 11 for the analytical model and for the model being derived from the PIO record and flight test data.

The reduction in the stick-free short period frequency from $\omega_{n_{sp}}' = 9.8$ to $\omega_{n_{sp}}' = 7.0$ rad/sec accounts for approximately 92° of the 174° difference in the δ_H/F_s phase angles shown in Figure 11. The next part of the transfer function to be reviewed was the stick-free feel system root. The Northrop reports state that the natural frequency of the feel system is primarily a function of the control system mass and feel spring. The natural frequency is appreciably higher than the PIO frequency, i.e., $\omega_{n_{F_s}} \approx 18$ rad/sec compared to 7.4 rad/sec so the phase shift contribution at 7.4 rad/sec is small. An adjustment to the feel system dynamics suggested in Reference 6 to account for the pilot's arm mass would reduce the natural frequency and damping ratio of the feel system to approximately $\omega_{n_{F_s}}' = 13$ rad/sec and $\zeta_{F_s} = 0.13$. These values were used in the δ_H/F_s transfer function (PIO record) on Figure 11 to estimate the phase contribution of the feel system. Using the experimental estimates of the stick-fixed and stick-free short period, the feel system and the δ_H/F_s phase angle from the PIO record, the phase contribution of the horizontal stabilizer servo is established as approximately 101° at $\omega = 7.4$ rad/sec.

The first order analytical model in Table 1 for the servo is (s =-21.7) which gives 18.7° phase lag at ω = 7.4 rad/sec. Obviously, the servo can not be described as a first order linear element if it exhibits more than 90° of phase shift. It is probable that the servo is higher order and possibly nonlinear.

With the above analysis pointing to the horizontal tail servo as a major contributor of phase lag, a search was made of reports for commentary, data, time histories, frequency responses, etc. relating to the servo. The transient response in Figure 12 for damper OFF was photographically enlarged and the stick deflection doublet was transformed, through the nonlinear gearing curve of Figure 14, into a horizontal tail command δ_{H_c} and plotted in Figure 15. The actual horizontal tail response is also plotted on Figure 15. This comparison shows large attenuation and phase shift for an input that has frequency content near 12 rad/sec. This transient response verifies that the servo is not a 21.8 rad/sec linear first order element. Note that in performing the doublet input, the pilot applied full aft stick commanding 15° of stabilizer deflection at a flight condition where the static load factor sensitivity is 2.32 g/deg. The horizontal stabilizer servo command and the horizontal stabilizer response to a similar doublet stick input is shown in Figure 15a for a test performed at high altitude and lower speed (i.e. lower dynamic pressure). This record indicates much less attenuation and smaller phase shift than the record taken at high dynamic pressure illustrated in Figure 15. These two responses suggest that the servo response is a function of hinge moments. Examination of the PIO time history in Figure 1 between 8-8.5 sec shows that the pilot applied a push-pull doublet of 34 lb push and 24 lb pull. It should be noted, however, that the peaks in the force application are phased so that the pilot-applied force and the bobweight force add. Thus, the total force applied to the feel spring is 37 lb push and 31 lb pull. Statically, these force applications, see Figure 16, would command 14° TED and 6° TEU of horizontal tail deflection. The frequency content of the doublet is roughly 10-15 rad/sec. If the analytical model of the servo actuator were correct, this command would have been followed with unity gain and small phase lag. The PIO record, however, indicates only 4° TED and 0.6° TEU response with considerable phase shift. This record also indicates that the servo has not been modeled correctly.

The dynamic characteristics of the horizontal tail servo are discussed in Reference 8 and curves relating servo valve flow as a function of valve displacement are presented,in Figure 17,for three valves that were under study. The flow characteristics of the valve used on airplanes with the PIO problem is not included on Figure 17. A frequency response performed on the controls test stand for the servo valve used on the production airplane with the PIO problem (Configuration D) is shown in Figure 18 for two levels of force input, $F_s = \pm 7$ lb and $F_s = \pm 15$ lb. These two frequency responses exhibit nonlinear response with amplitude and considerable reduction in the value of the first order root in the third order model used to fit the test data. It is most probable that the servo valve flow is a function of load pressure as indicated in Figure 19. The parabolic curves in Figure 19 are typical of hydraulic flow control valves. When the load pressure becomes a large fraction of the supply pressure, the gradient of flow output with valve displacement is reduced and the dynamic response of the servo is degraded, however, the servo is capable of passing low frequency inputs and holding static loads as long as the load pressure does not exceed the system supply pressure. Reference 4 states on page 122 that the surface deflection rates are a function of the air load hinge moments.

Commentary and evaluation data from simulator experiments indicated that tests of a servo valve with time constant reduced by 1/2 resulted in "definitely reduced PIO tendencies with no degradation in flying qualities". The flight test program performed to evaluate various changes to the flight control system is described in Reference 1. Table 1 from that report documents the chronology of modifications evaluated. Note that the new servo valve was introduced in Mod I and by Mod IV most of the control system changes that were eventually adopted to fix the PIO problem had been introduced, i.e., trigradient spring, reduced bobweight, reduced preload, new servo valve. Only the change to the nonlinear gearing had not yet been made. In Mod VI the original servo valve was reinstalled. The evaluation comments were as follows (from page D-27 of Reference 1): "The pilot evaluated Mod VI no better than the baseline control system for both PIO and Cooper ratings. The control system performance deterioration was so distinct that only one flight was made with this configuration". This test indicates that the major cause of the PIO problem was the low dynamic performance of the servo.

The question might be asked – "Why spend time analyzing a problem that was adequately solved fifteen years ago?" The reason the study was performed was because the T-38A PIO incident has been used by a number of researchers to test their theories for what causes pilot-induced oscillations. In referring to the incident, however, they all use the analytical model developed in Reference 6 to represent the airplane. This model is incorrect and therefore analysis based on the analytical model or correlation of PIO theories with the parameters in the analytical model such as those in References 3, 4 and 5 are invalid.

REFERENCES

1. Finberg, F., Lt./Col.: "Report of the T-38 Flight Control System Pilot Induced Oscillation (PIO) Review Board," Aeronautical System Division, Wright-Patterson Air Force Base, Ohio, 15 February 1963.

2. Hirsch, D. L.: "Investigation and Elimination of PIO Tendencies in the Northrop T-38A," paper presented at the SAE Meeting, July 1964, New York, Northrop Norair.

3. Ashkenas, I. L., Jex, H. R. and McRuer, D. T.: "Pilot-Induced Oscillations: Their Cause and Analysis," Norair Report NOR-64-143, Systems Technology, Inc. Report STI TR-239-2, 20 June 1964.

4. SRL, Inc.: "A Theory for Longitudinal Short-Period PIO," Technical Report No. AFFDL-TR-77-57, Interim Report for period November 1975 - April 1977, May 1977.

5. Chalk, C. R., Neal, T. P., Harris, T. M. and Pritchard, F. E.: "Background Information and User Guide for MIL-F-8785A(ASG) "Military Specification - Flying Qualities of Piloted Airplanes," prepared for AFFDL, June 1969.

6. Jex, H. R.: "Summary of T-38A PIO Analyses," STI TM No. 239-3, 25 January 1963.

7. Schubert, G. R.: "Digital Computer Program for Root Locus Analyses of Open-Loop Transfer Functions Containing an $e^{-\tau s}$ Lead-Lag Term," AFFDL FDCC TM 65-43, September 1965.

8. Nelson, W. E.: "An Analytical Investigation for the Possible Optimization of the T-38A Longitudinal Control System," Northrop Norair Report No. NOR-64-52 (FMR-61-2), February 1964.

9. Lusby, W. A., Jr., and Hanks, N. J.: "T-38A Category II Stability and Control Tests", Report No. AFFTC-TR-61-15, August 1961.

Table 1

T-38A STICK-FREE TRANSFER FUNCTIONS

$$\frac{\theta}{F_s} = \frac{.0084\left[\frac{s}{3.18}+1\right]}{s\left[\frac{s}{21.8}+1\right]\left[\frac{s^2}{9.8^2}+\frac{2(.10)}{9.8}s+1\right]\left[\frac{s^2}{17.7^2}+\frac{2(.23)}{17.7}s+1\right]}$$

$$\left.\frac{n_z}{F_s}\right|_{\substack{K_B=2.0 \\ F.S.=200}} = \frac{.248\left[\frac{s^2}{24.4^2}+\frac{2(.17)}{24.4}s+1\right]}{\left[\frac{s}{21.8}+1\right]\left[\frac{s^2}{9.8^2}+\frac{2(.10)}{9.8}s+1\right]\left[\frac{s^2}{17.7^2}+\frac{2(.23)}{17.7}s+1\right]}$$

Flight Condition

M = .85 ~ .90 C.G. = 16%

h = S.L.~ 5,000 ft W = 11,690 lb

F.S. = 200 is pilot station

Table 2

PILOT MODELS THAT CAUSE ROOT LOCI
TO BECOME UNSTABLE AT ω = 7.4 AND 19.6 RAD/SEC

NO. 1

$$Y_p = \frac{184.2\left[\frac{s^2}{12.54^2} + \frac{2(.03064)}{12.54}s + 1\right]}{\left[\frac{s^2}{18.6^2} + \frac{2(.14)}{18.6}s + 1\right]} e^{-.239s}\Big|_{\omega = 7.4} = 141.4\, e^{-108.4^\circ j}$$

NO. 2

$$Y_p = \frac{372.3\left[\frac{s^2}{10.37^2} + \frac{2(.16)}{10.37}s + 1\right]}{\left(\frac{s}{5.5} + 1\right)\left[\frac{s^2}{18.6^2} + \frac{2(.14)}{18.6}s + 1\right]} e^{-.164s}\Big|_{\omega = 7.4} = 141.54\, e^{-105.5^\circ j}$$

NO. 3

$$Y_p = \frac{11.45\left(-\frac{s}{.540} + 1\right)\left(\frac{s}{9.574} + 1\right)}{\left(\frac{s}{5.5} + 1\right)\left(\frac{s^2}{18.6^2} + \frac{2(.14)}{18.6}s + 1\right)} e^{+.015s}\Big|_{\omega = 7.4} = 139.7\, e^{-102.7^\circ j}$$

NO. 4

$$Y_p = \frac{K_\theta\,(.0084)\left[\frac{s^2}{11^2} + \frac{2(.32)}{11}s + 1\right]}{\left[\frac{s^2}{18.6^2} + \frac{2(.14)}{18.6}s + 1\right]} e^{-.0957s}$$

$[n_z, \theta, \theta$ feedback$]$

TABLE I

Mod. No	CONTROL SYSTEM CHANGE	EOC No.	Test Flight No.
0	Baseline T-38A Control System A. Spring Gradient dF_s/dT_s=4.5 lb/in) See Fig. 3 Spring Preload F_p=1.25 lb. B. Total Bob-weight effectiveness dF_{BW}/dT_s=1.7 lb/g at δH=1° T.E. UP. See Fig. 6		162 thru 168 incl.
I	A. Increased stick force spring gradient-See Fig. 3 to dF_s/dT_s = 10 lb/in Flt. 169 Spring Preload F_p=0.5 lb. at stick grip Flt. 172 Spring Preload F_p=1.6 lb. at stick grip B. New Servo-Valves with reduced time constant 1/2 that of production servo-valves	74519 74270 69999	169 thru 172 incl.
II	A. Stick force spring gradient changed-See Fig. 3 to dF_s/dT_s=7.0 lb/in Spring Preload F_p=0.8 lb. at stick grip B. Reduced Bob-Weight effectiveness to 1/2 T-38A 1. Modification of Bob-Weight Mechanism-See Fig 6 2. Removal of Aft Control Stick 3. Replace Bob-Wt. Balance Spring C. New Servo-Valves (Mod I)	74519 74540 74552 74548 Noted	174 thru 177 incl.
III	A. Tri-Gradient Control Force Spring-See Fig. 4 Gradient #1 dF_s/dT_s= 10 lb/in #2 dF_s/dT_s= 8.5 lb/in #3 dF_s/dT_s= 7 lb/in Spring Preload F_p= 0.15 lb. at stick grip B. Reduced Bob-Weight Effect (Mod II-B) C. New Servo-Valves (Mod I-B) ?	74579 74593 74594 Noted Noted	179 thru 181 incl.
IV	A. Tri-Gradient Spring-See Fig. 4 Gradient #1 dF_s/dT_s= 16 lb/in to F_{s1}= 1.5 lb #2 dF_s/dT_s= 11.8 lb/in to F_{s2}= 2.7 lb #3 dF_s/dT_s= 7.6 lb/in Spring Preload F_p= 0.5 lb. at stick grip B. Reduced Bob-Weight Effect (Mod II) C. New Servo-Valves (Mod I)	74580 75615 74579 75621 Noted Noted	182 and 184 only
V	Same as Mod IV, except Removed Bob-Weight Balance Spring	75624	183 only
VI	Same as Mod IV, except Replaced Production Servo-valves (Bob-Wt. Balance Spring Re-Installed)	75624	185 only

TABLE I Control System Test Modifications on aircraft AF 60-602 (N5115) for PIO Flight Test Program.
Sheet 1 of 2

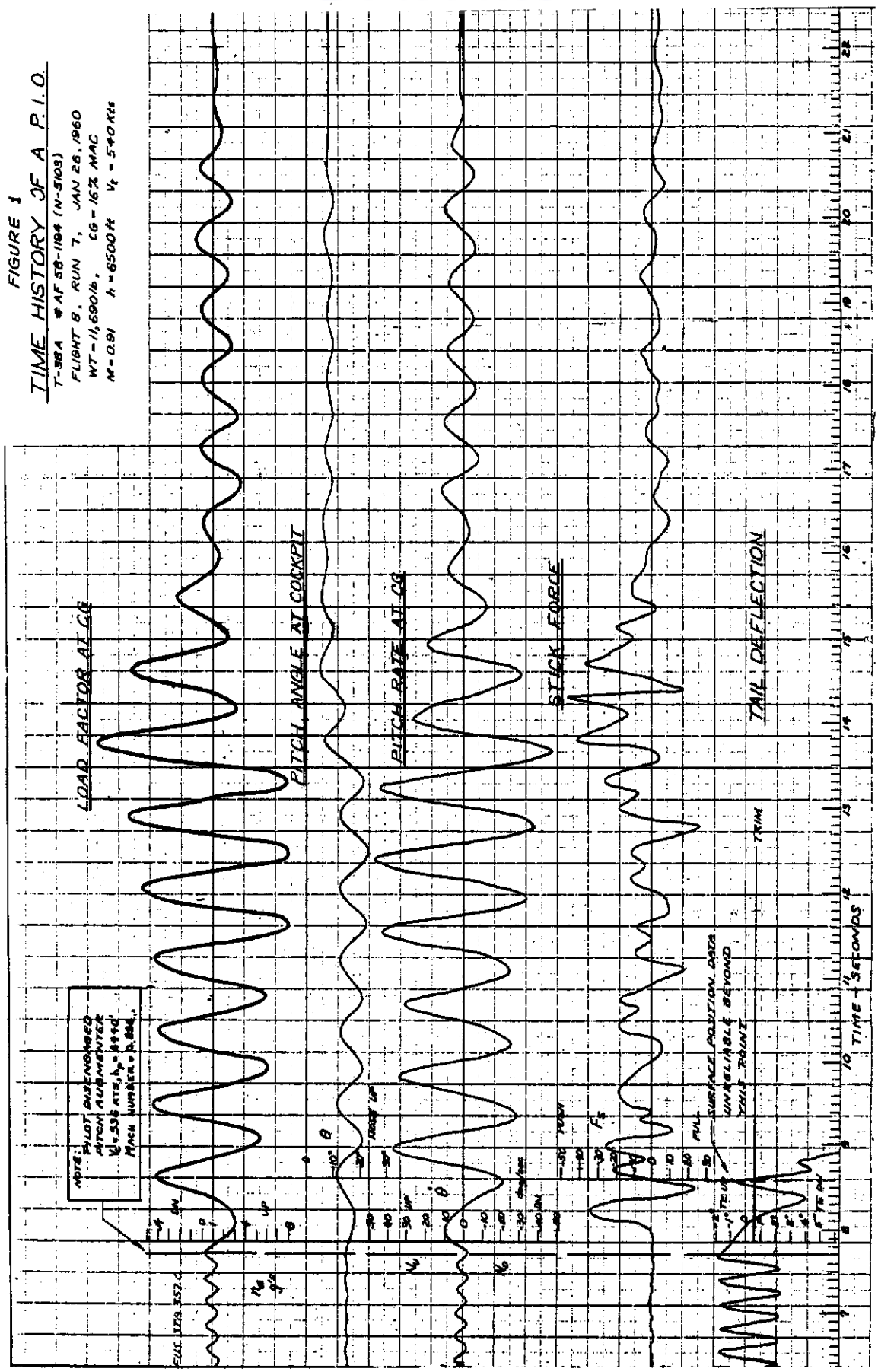

Figure 1 TIME HISTORY OF A P.I.O.

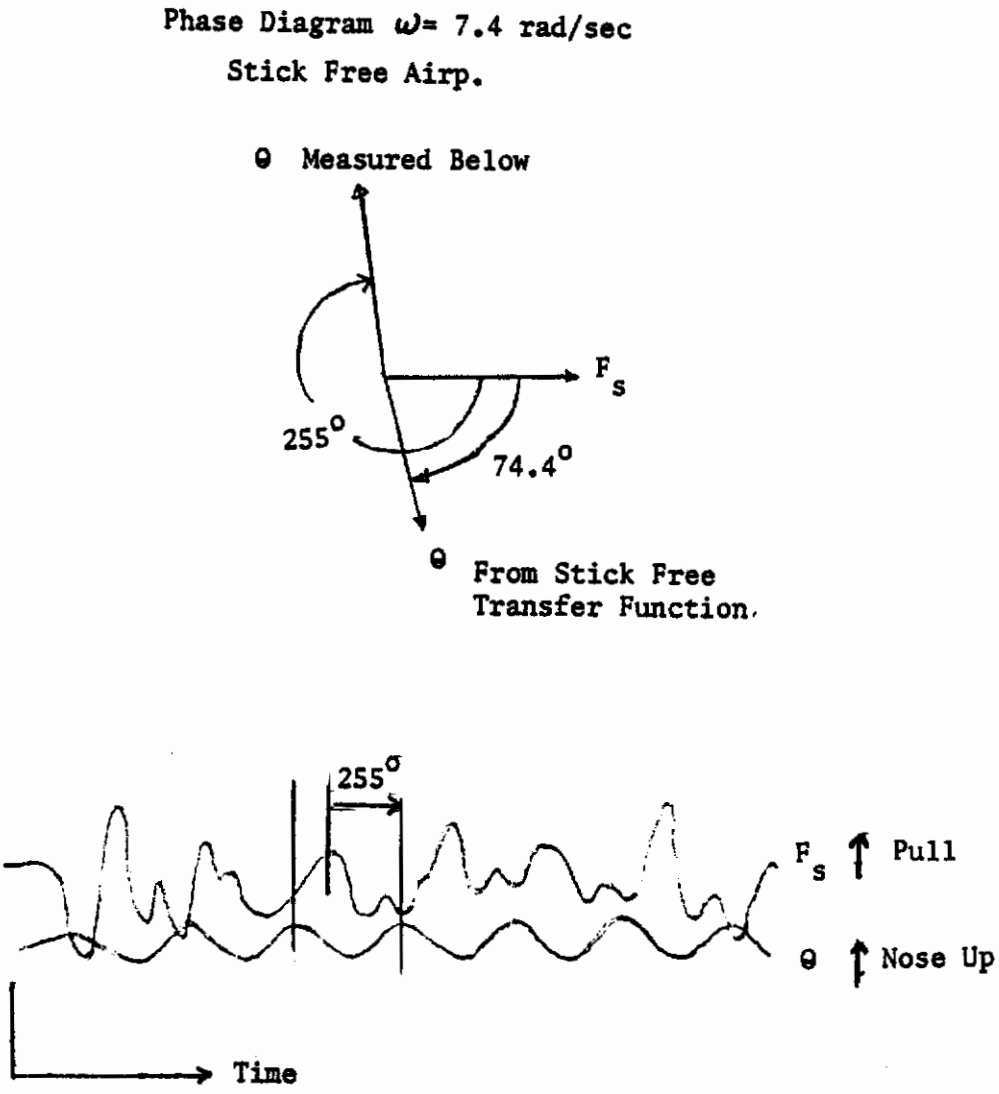

Figure 2 T-38A PIO TIME HISTORY AND ANALYTICAL MODEL PHASE ANGLE COMPARISON

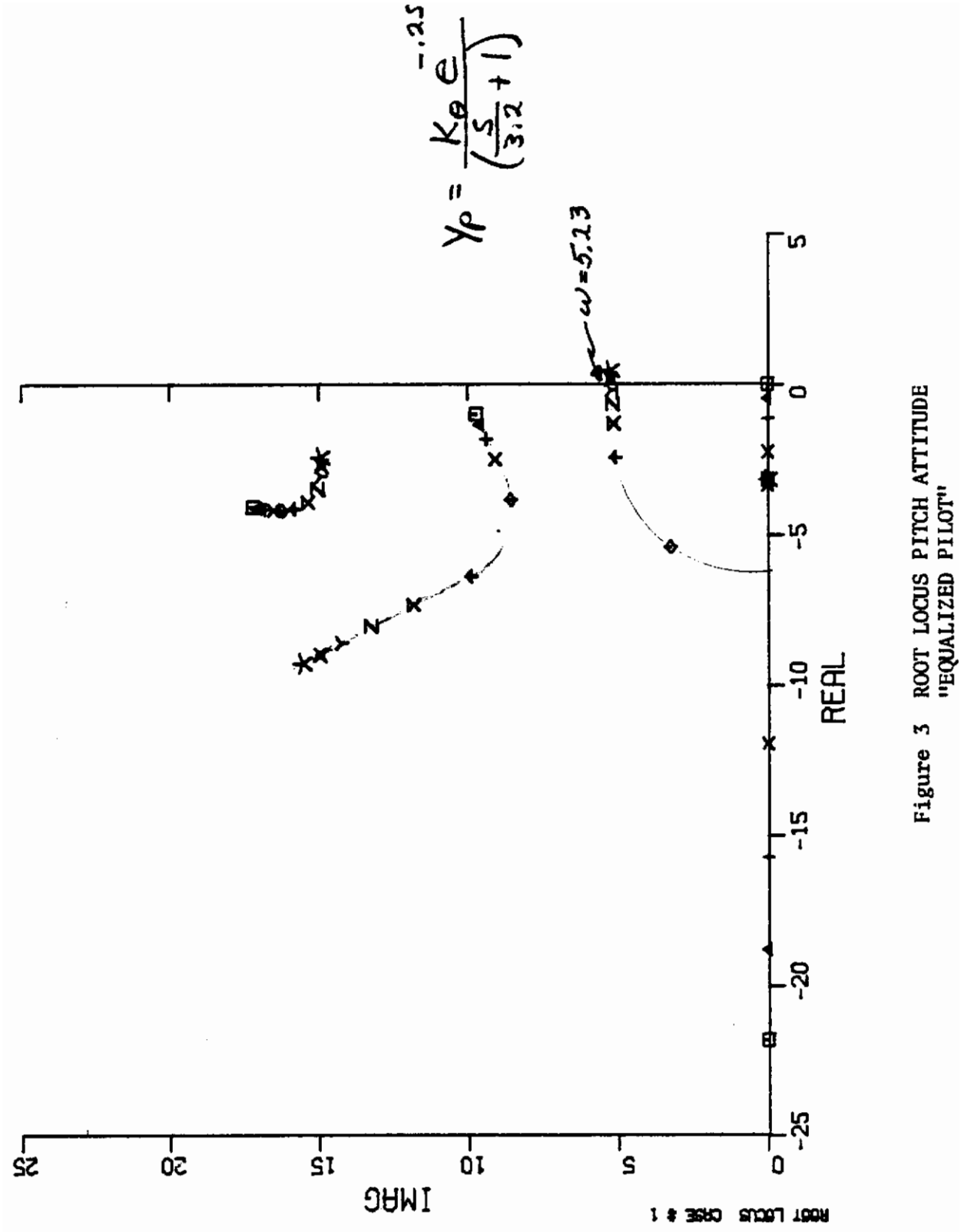

Figure 3 ROOT LOCUS PITCH ATTITUDE "EQUALIZED PILOT"

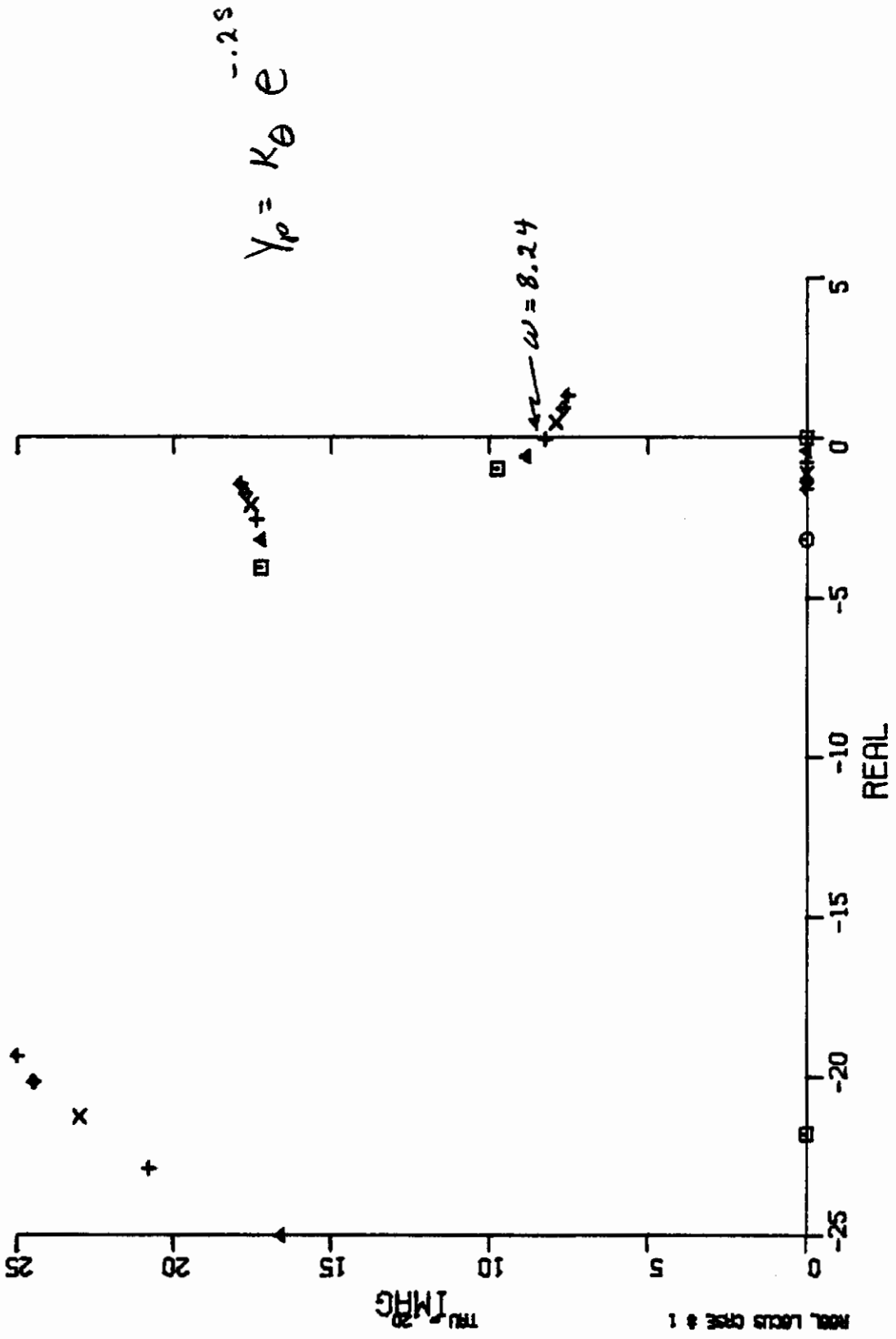

Figure 4 ROOT LOCUS PITCH ATTITUDE "PRIMITIVE PILOT"

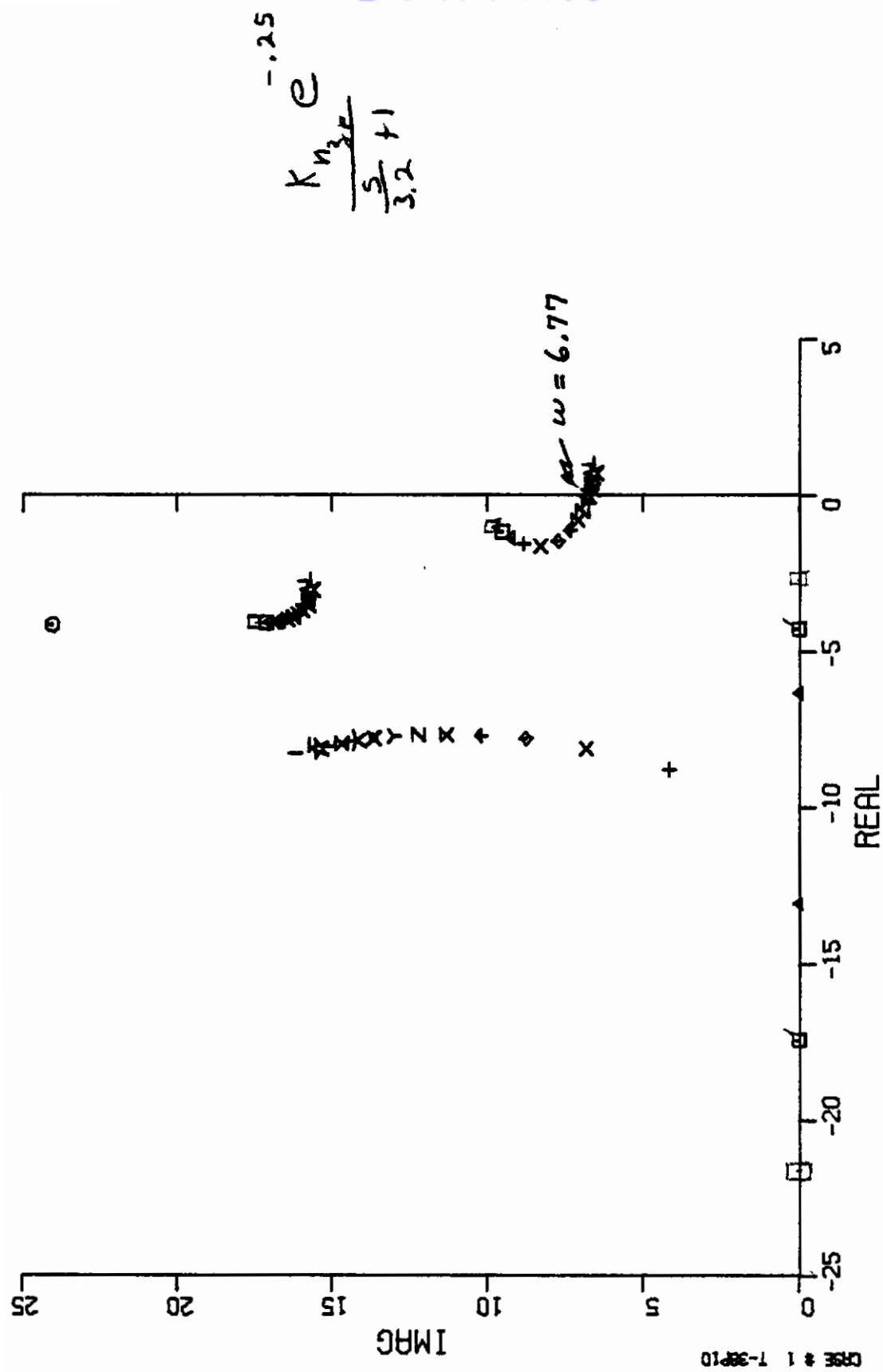

Figure 5 ROOT LOCUS NORMAL ACCELERATION "EQUALIZED PILOT"

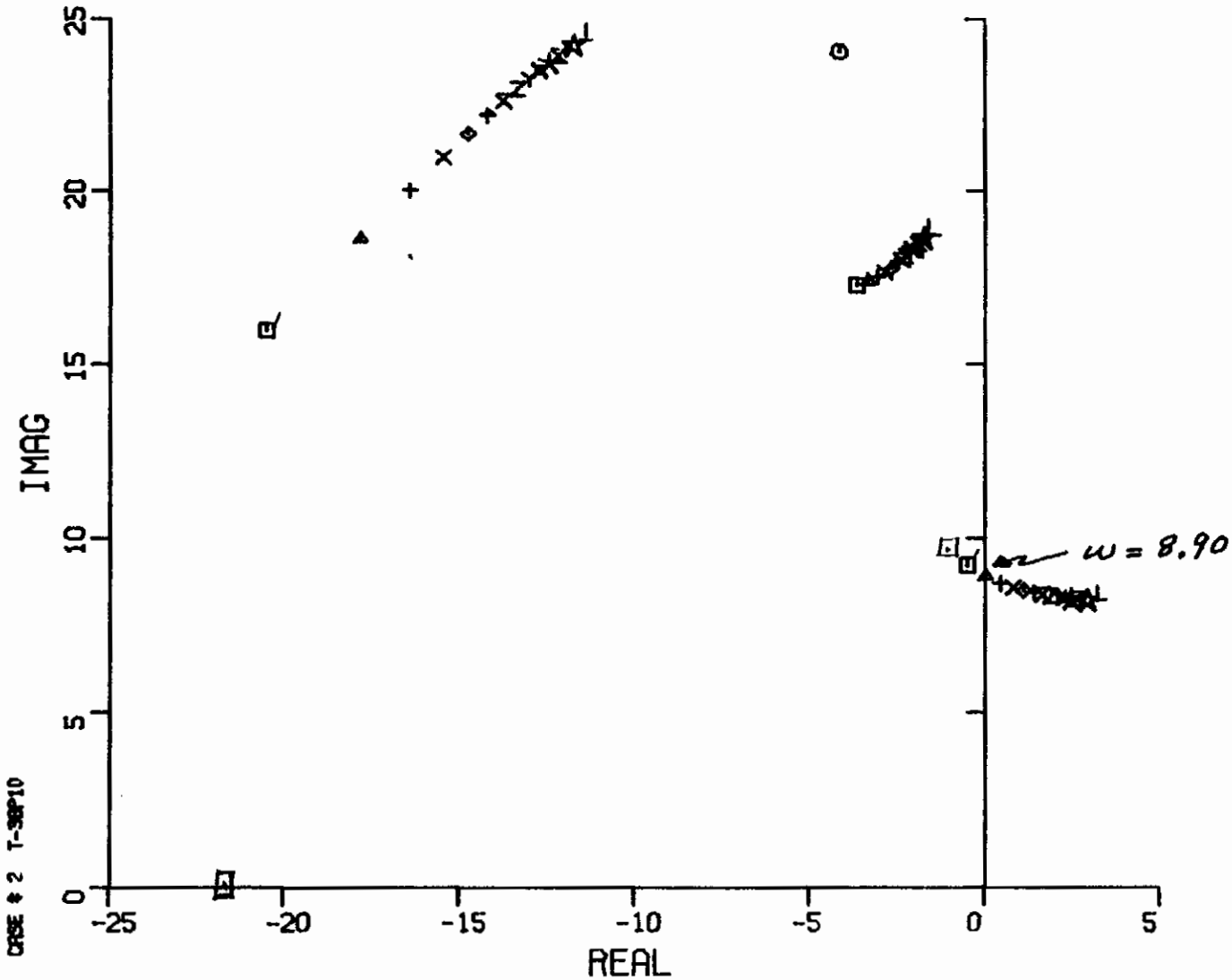

$K n_{z_{\delta p}} e^{-.2s}$

Figure 6 ROOT LOCUS NORMAL ACCELERATION
"PRIMITIVE PILOT"

$$\gamma_\rho = \frac{K_\theta \left[\frac{s^2}{12.542^2} + \frac{2(.03064)}{12.542}s+1\right]^{-.2395} e}{\left[\frac{s^2}{18.6^2} + \frac{2(.14)}{18.6}s+1\right]}$$

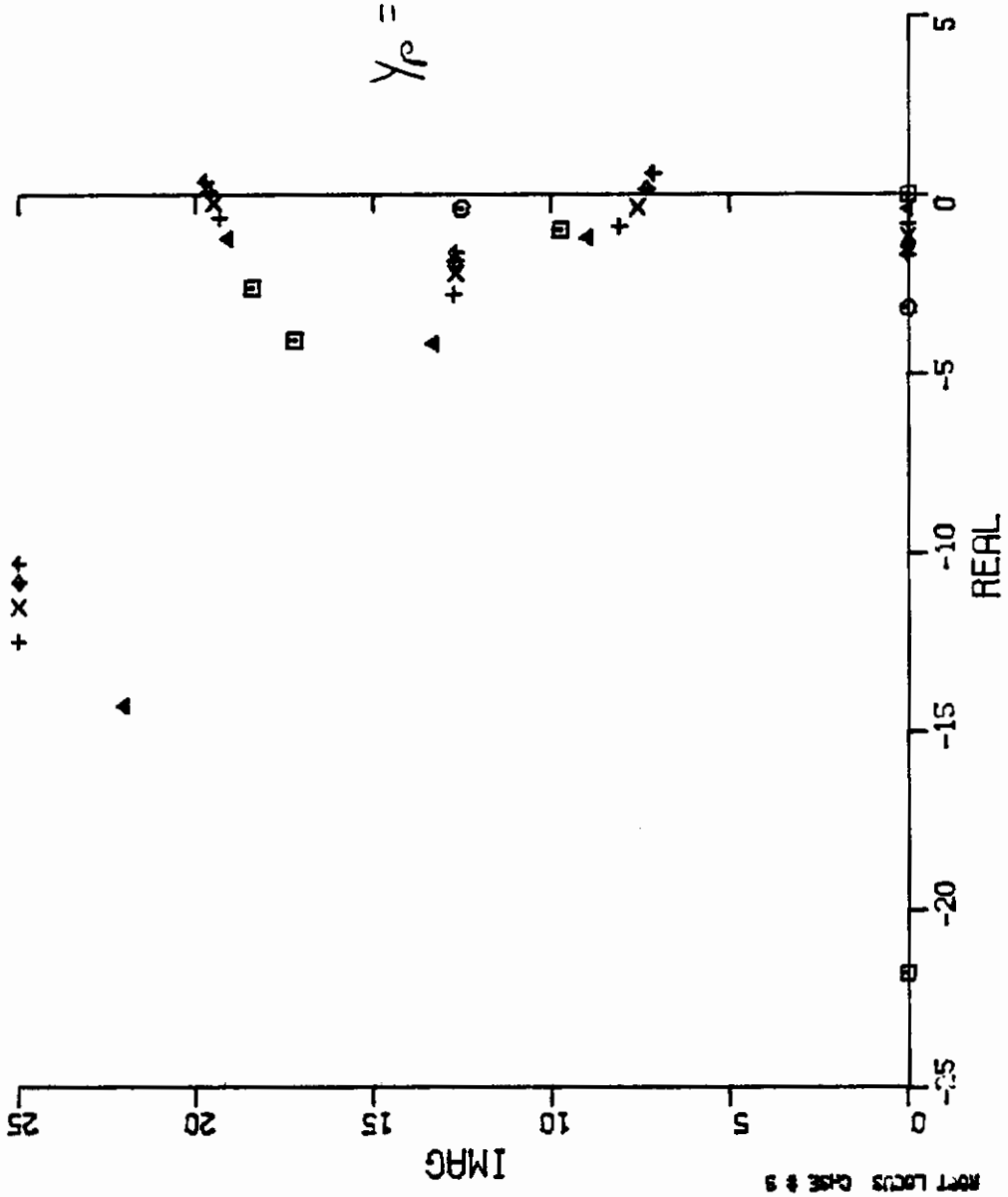

Figure 7 ROOT LOCUS FOR PILOT MODEL NO. 1

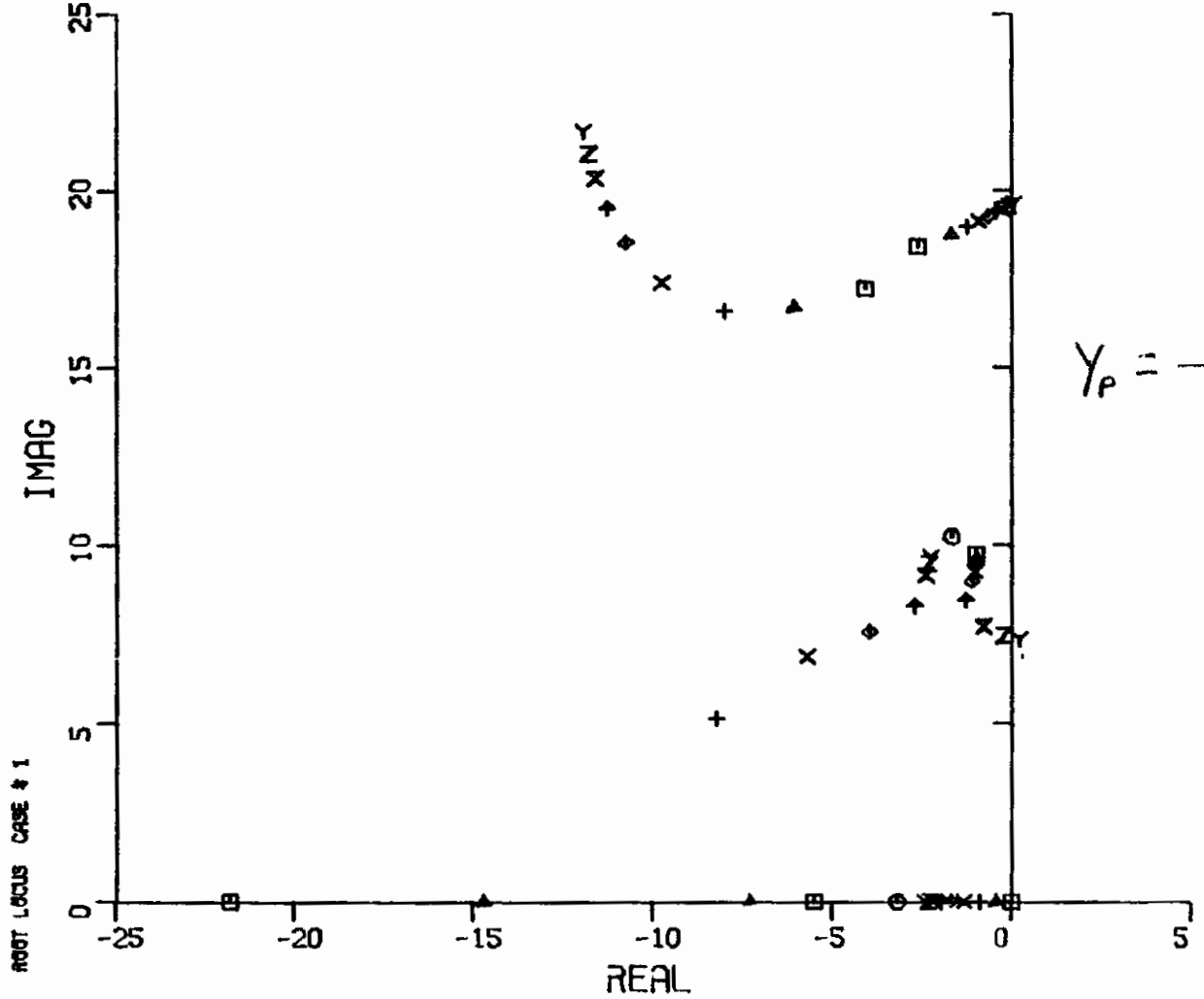

$$Y_p = \frac{K_\Theta\left[\frac{s^2}{10.372^2} + \frac{2(.16)}{10.372}s + 1\right]e^{-.1645s}}{\left(\frac{s}{5.5}+1\right)\left[\frac{s^2}{18.6^2} + \frac{2(.14)}{18.6}s + 1\right]}$$

Figure 8 ROOT LOCUS FOR PILOT MODEL NO. 2

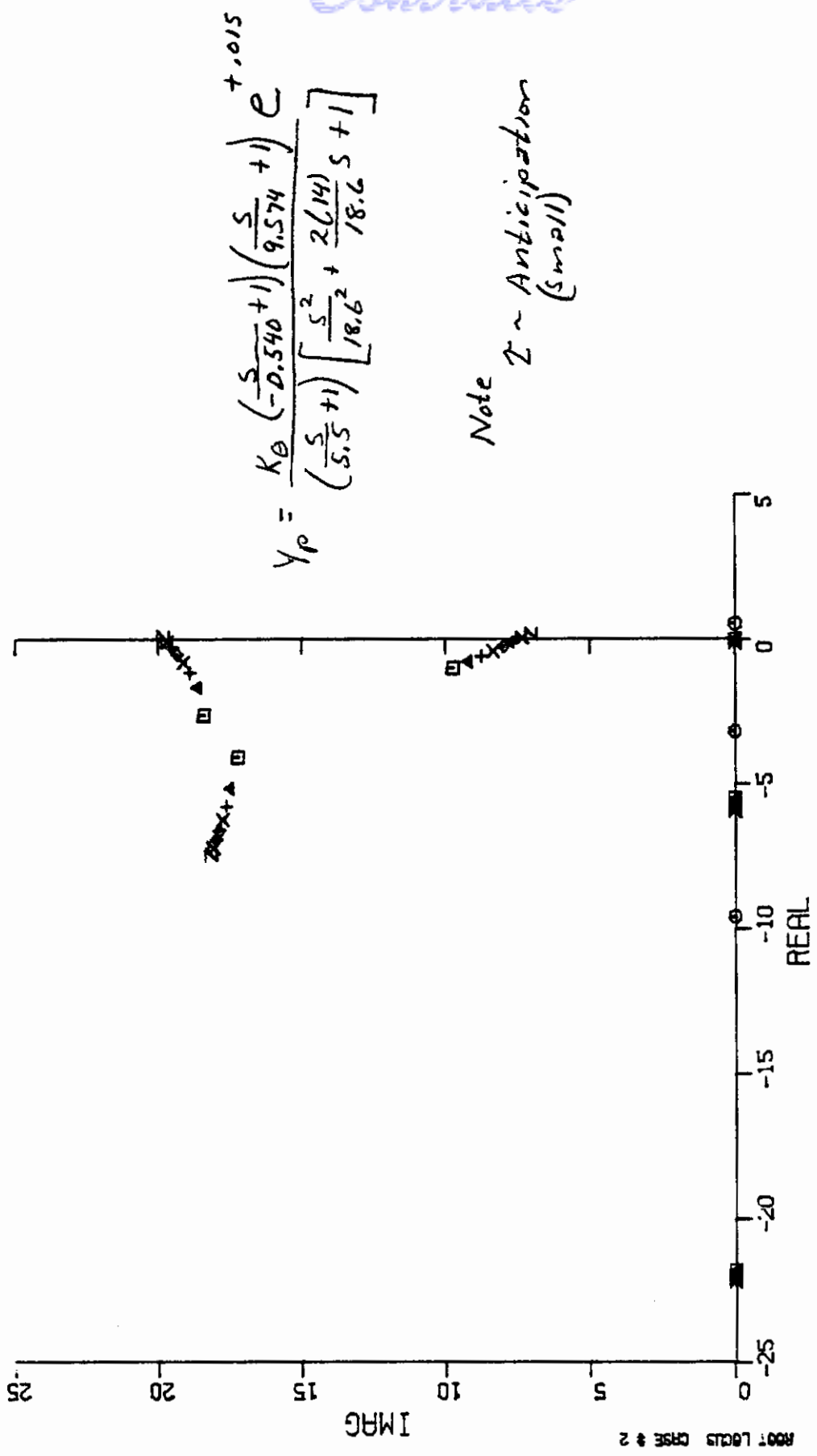

Figure 9 ROOT LOCUS FOR PILOT MODEL NO. 3

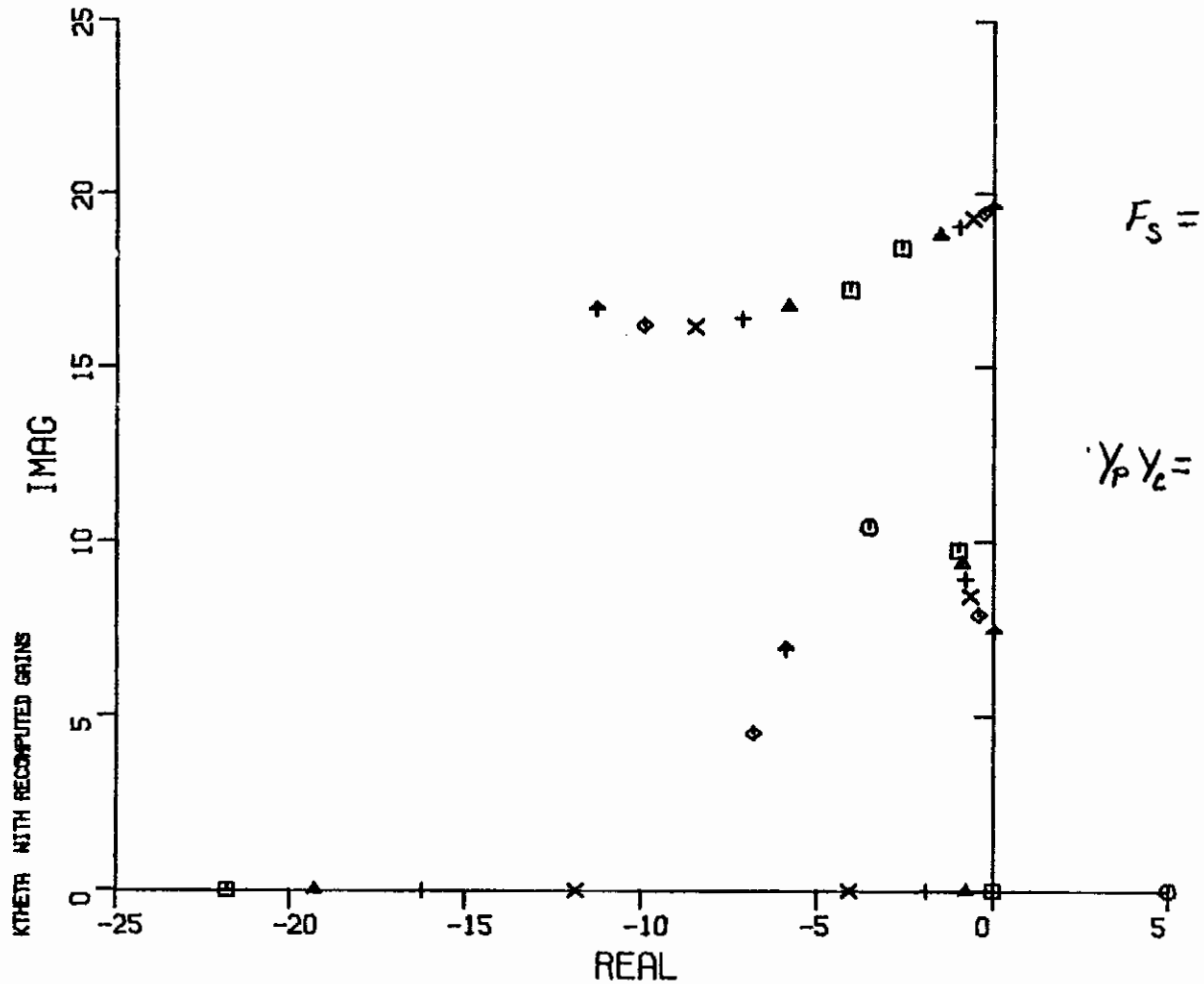

$$F_S = \frac{\left[K_{n_z} n_{z_\epsilon} + K_\theta \theta_\epsilon + K_{\dot\theta} \dot\theta_\epsilon\right] e^{-.2s}}{\left[\frac{s^2}{18.6^2} + \frac{2(.14)}{18.6} s + 1\right]}$$

$$Y_p Y_c = \frac{K_\theta (1.0084)\left[\frac{s^2}{11^2} + \frac{2(.32)}{11} s + 1\right] e^{-.09575s}}{\left[\frac{s^2}{18.6^2} + \frac{2(.14)}{18.6} s + 1\right] \quad \Delta_{T\text{-}38A}}$$

Figure 10 ROOT LOCUS FOR PILOT MODEL NO. 4

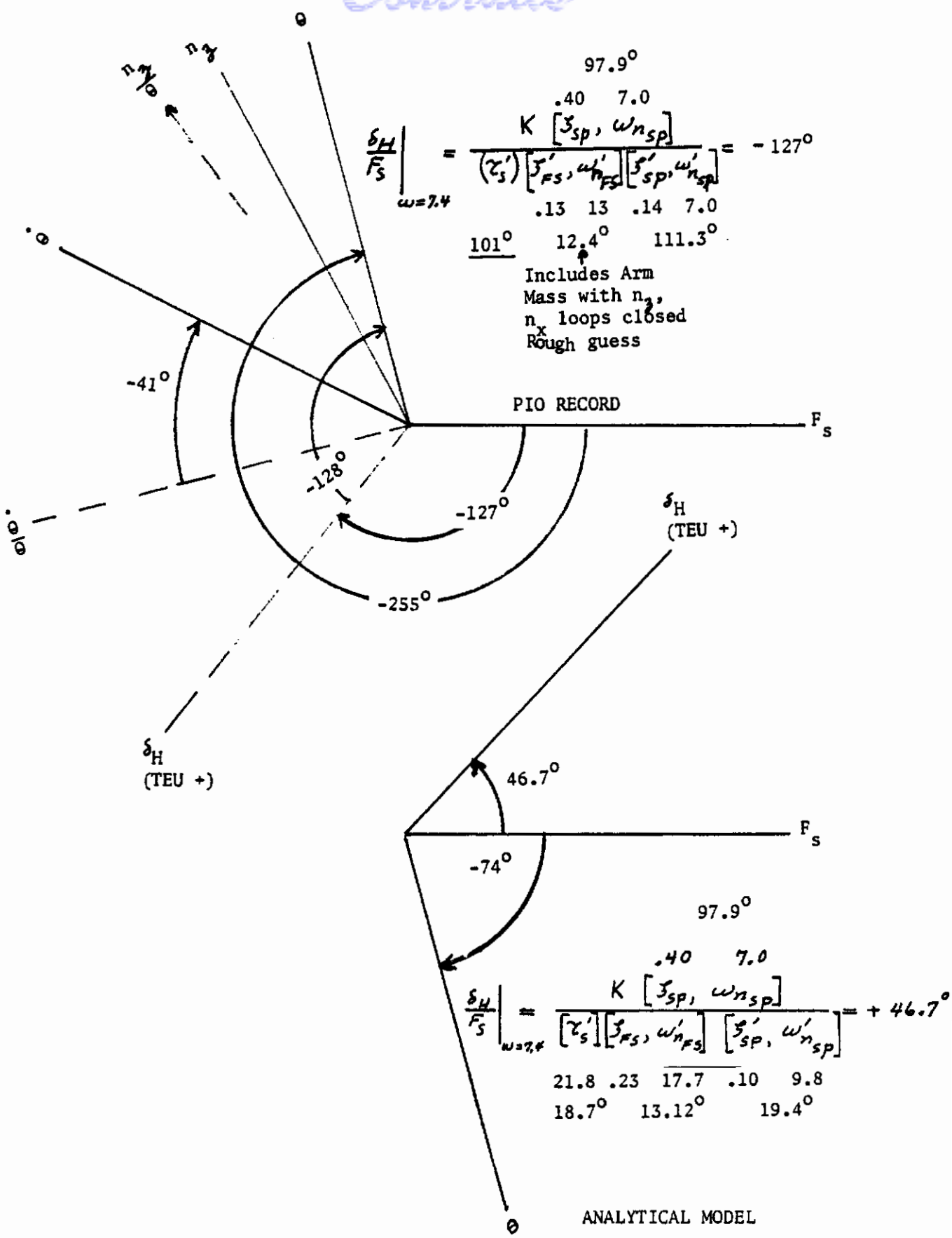

Figure 11 PHASE RELATION OF PIO TIME HISTORIES

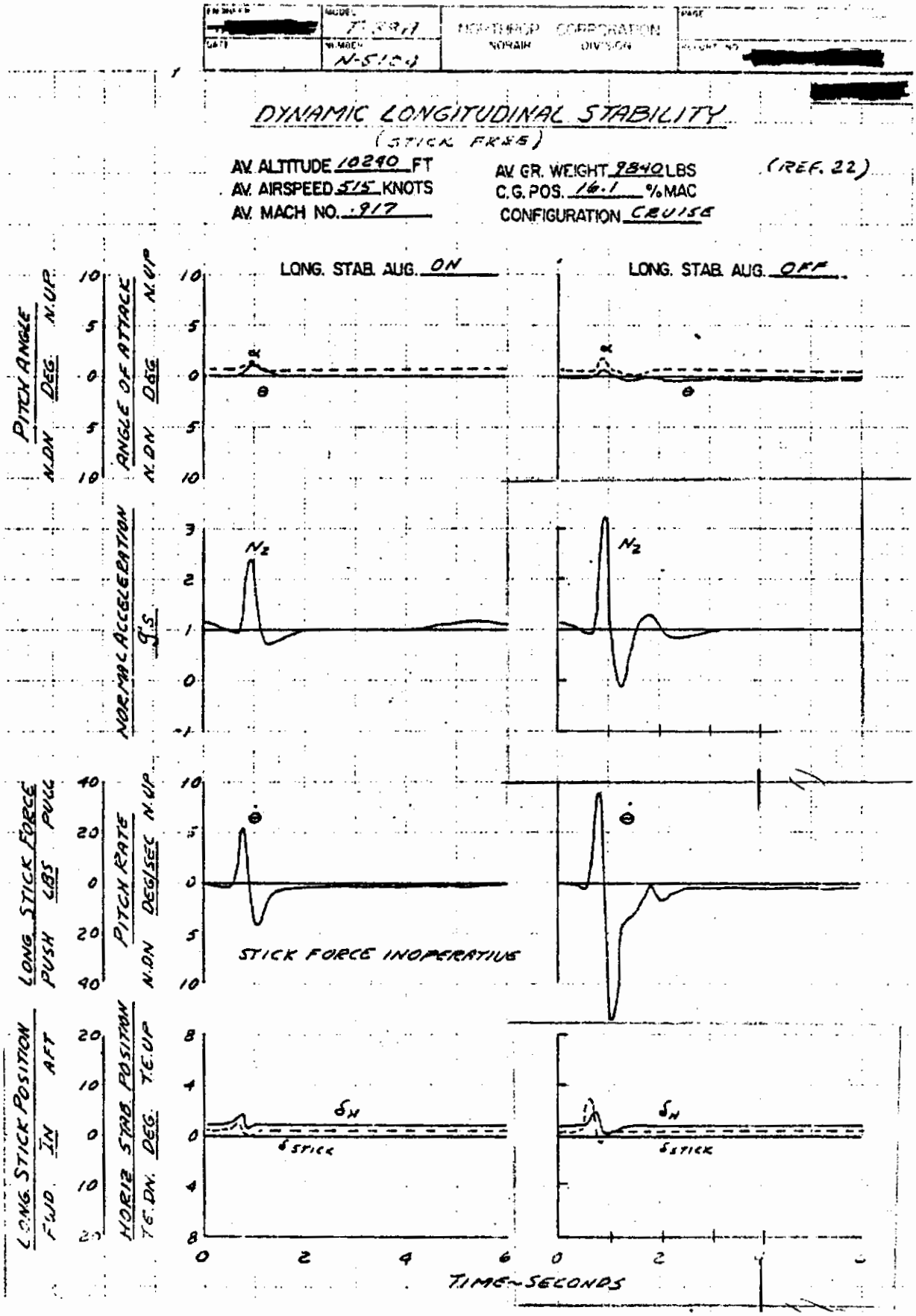

Figure 12 DYNAMIC STABILITY TEST ~ STICK FREE

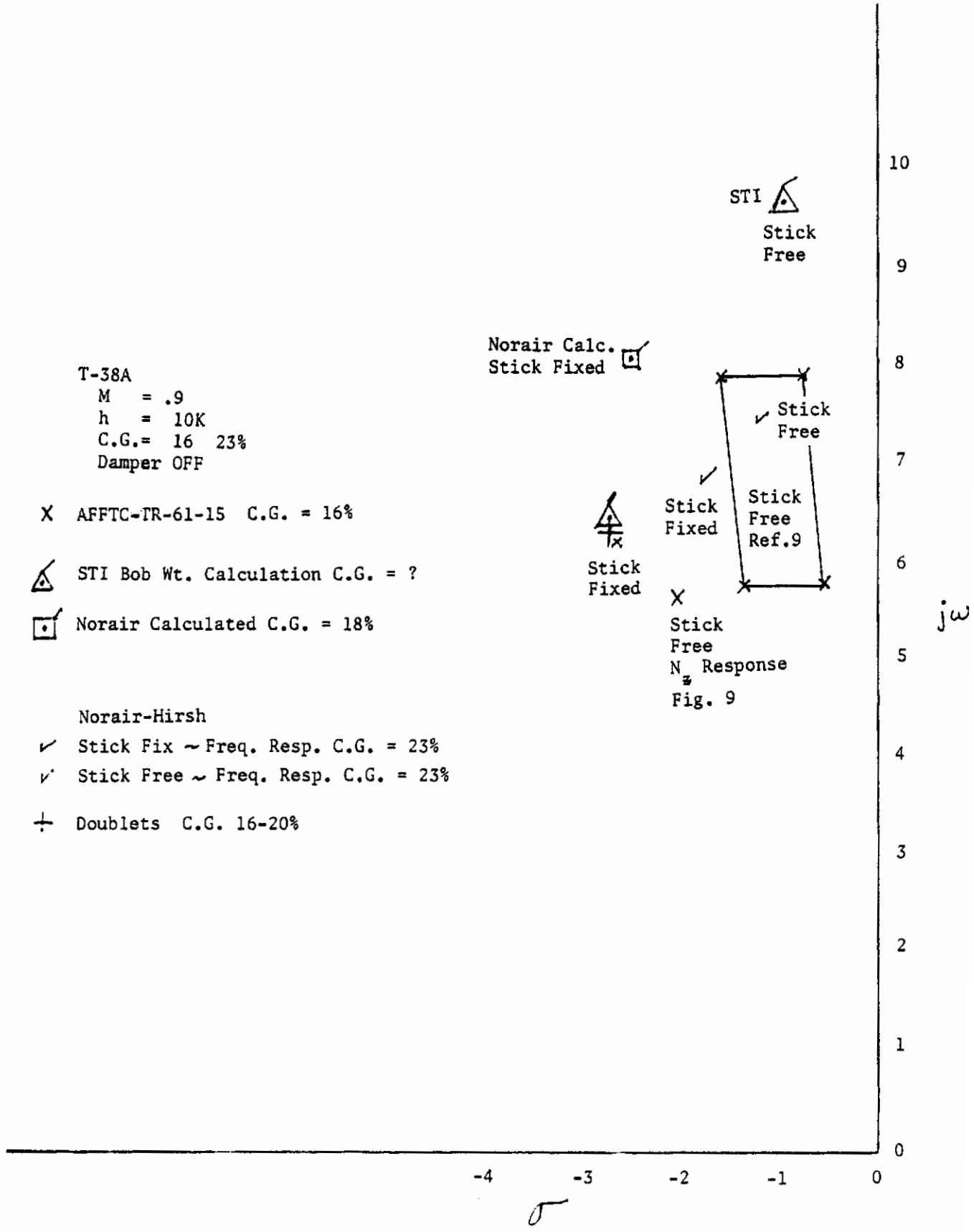

Figure 13 T-38A SHORT PERIOD DYNAMICS

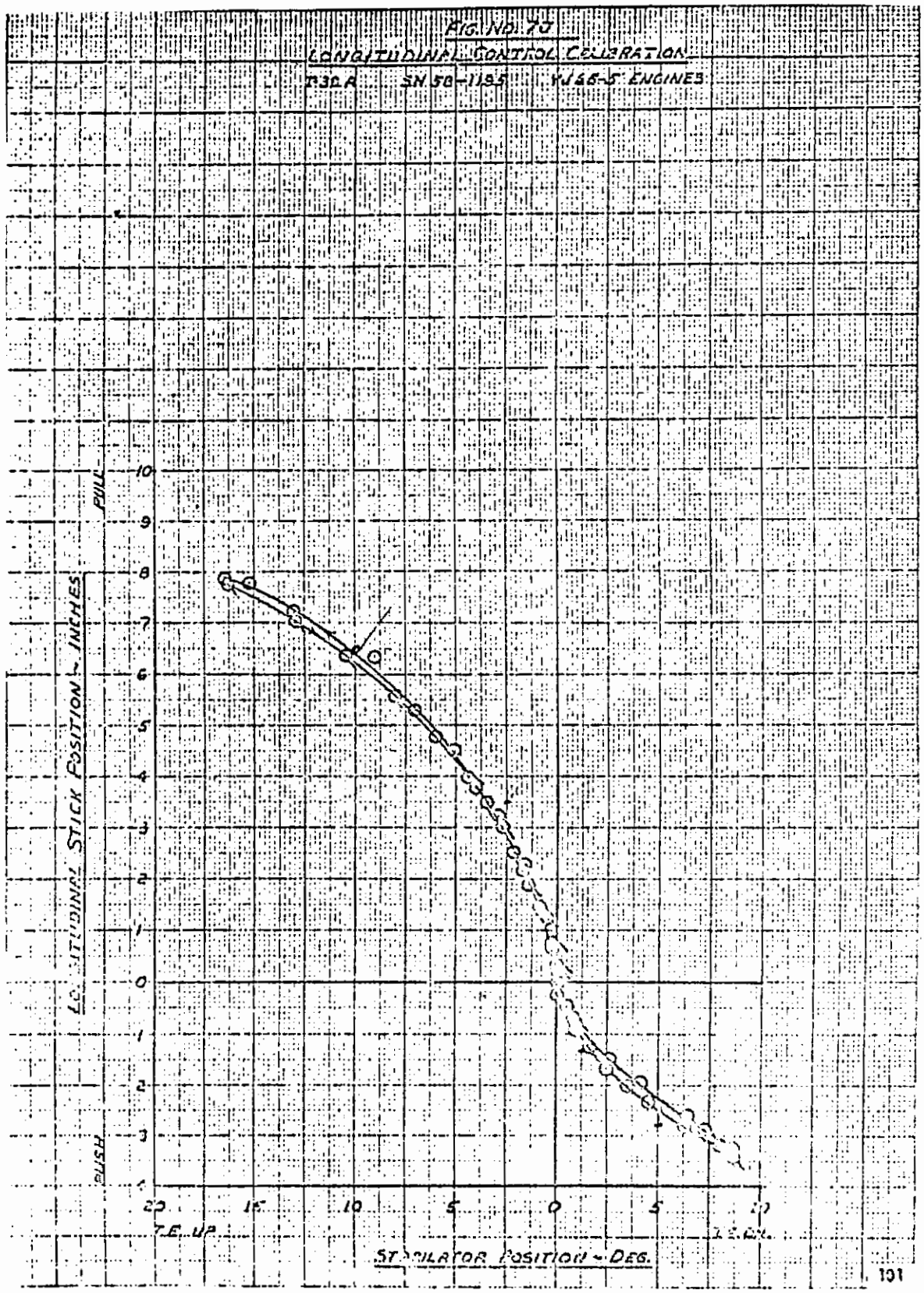

Figure 14 NONLINEAR CONTROL GEARING

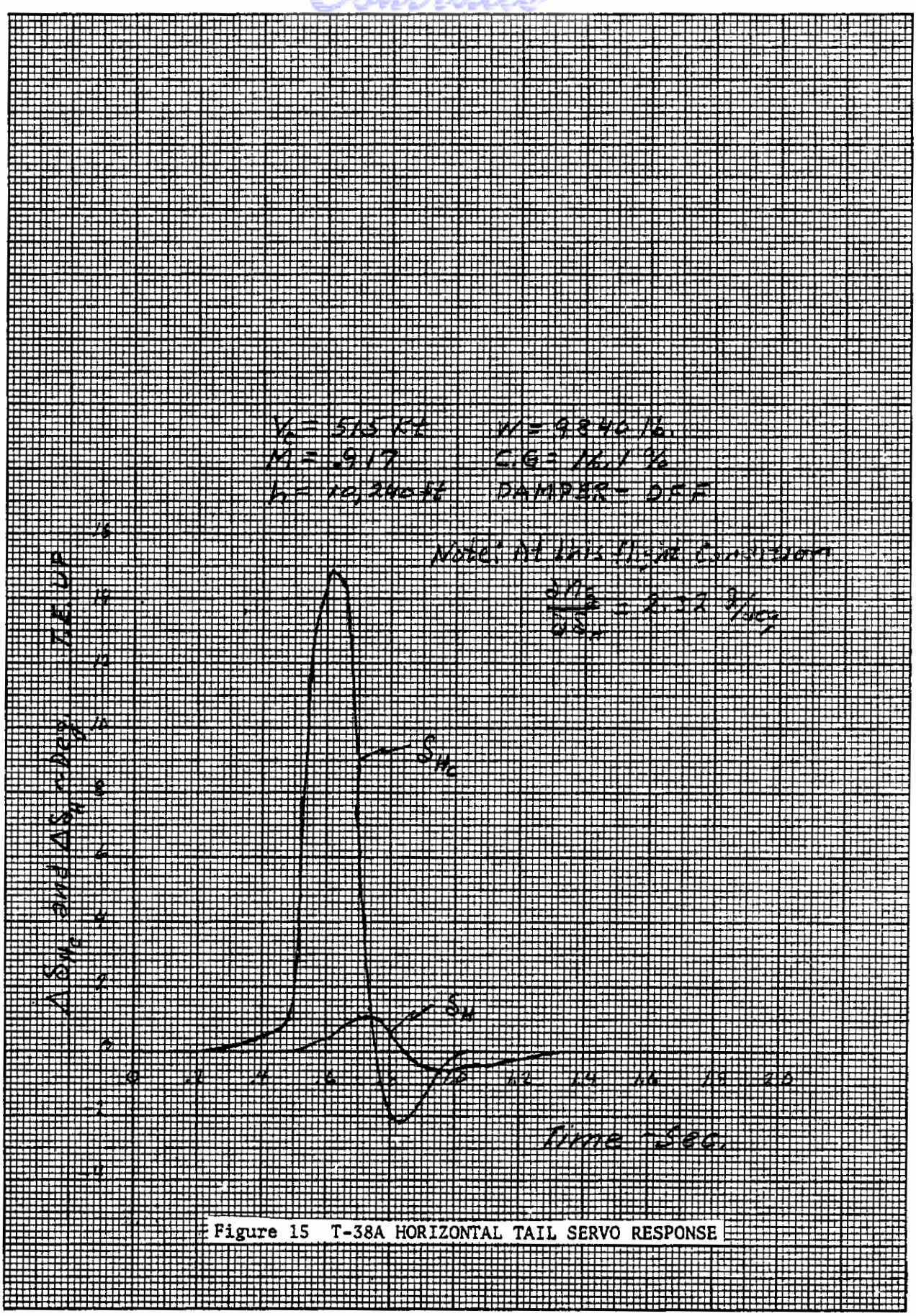

Figure 15 T-38A HORIZONTAL TAIL SERVO RESPONSE

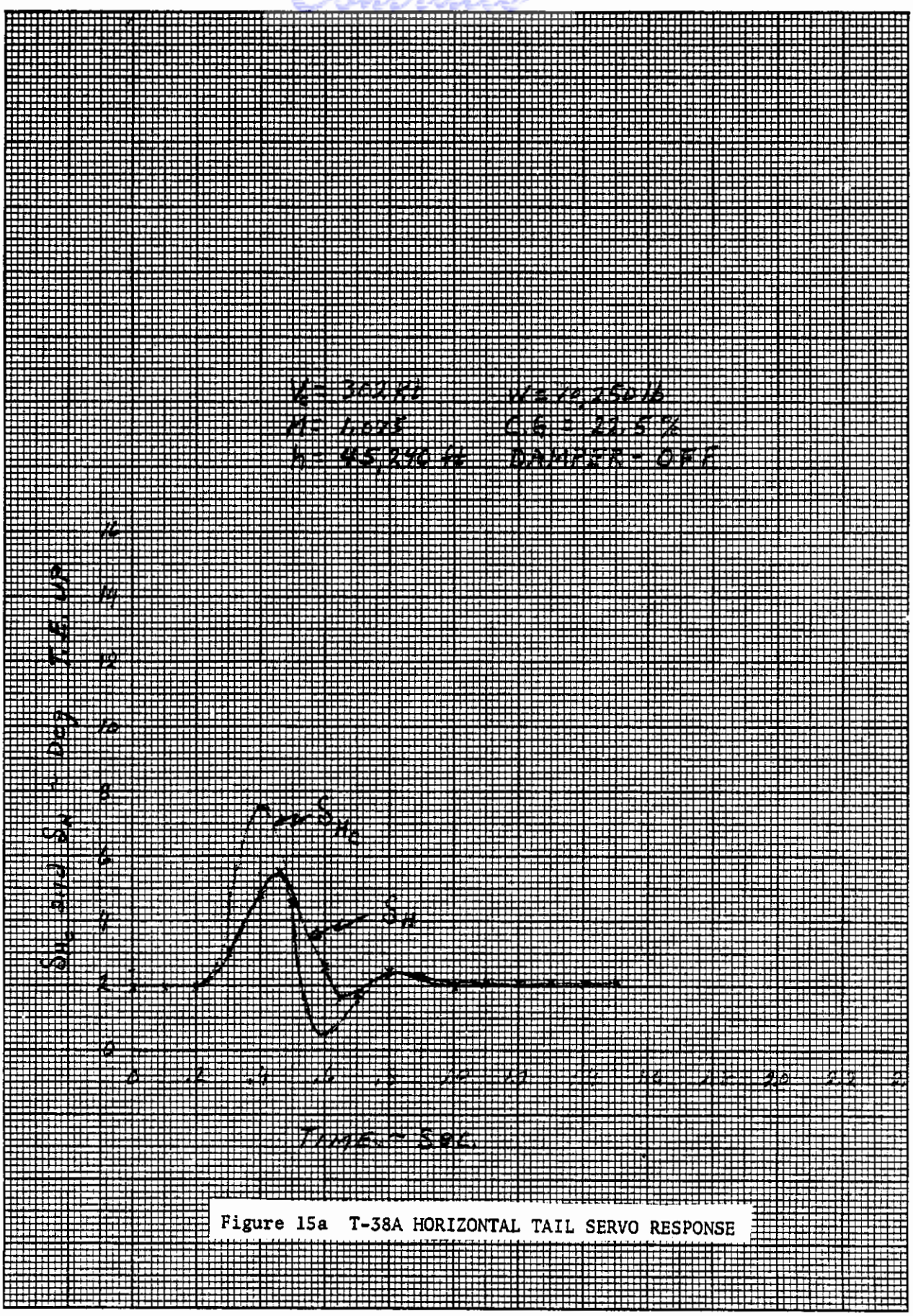

Figure 15a T-38A HORIZONTAL TAIL SERVO RESPONSE

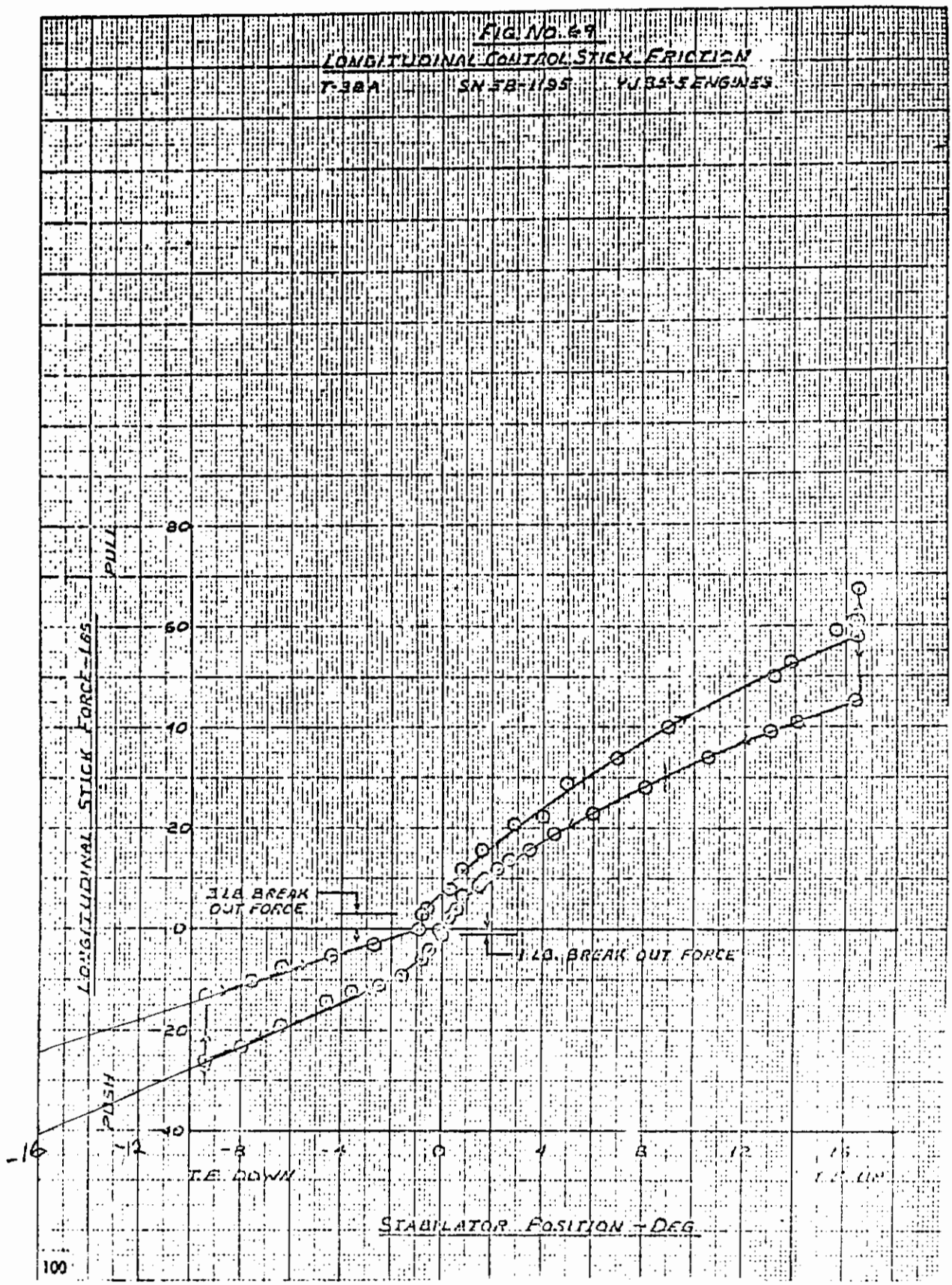

Figure 16 STICK FORCE (APPLIED TO FEEL SPRING) VS. STABILATOR POSITION

HYDRAULIC FLOW RATE OF THE LONGITUDINAL
CONTROL SYSTEM SERVO VALVES
(Based on Test Bench Data)

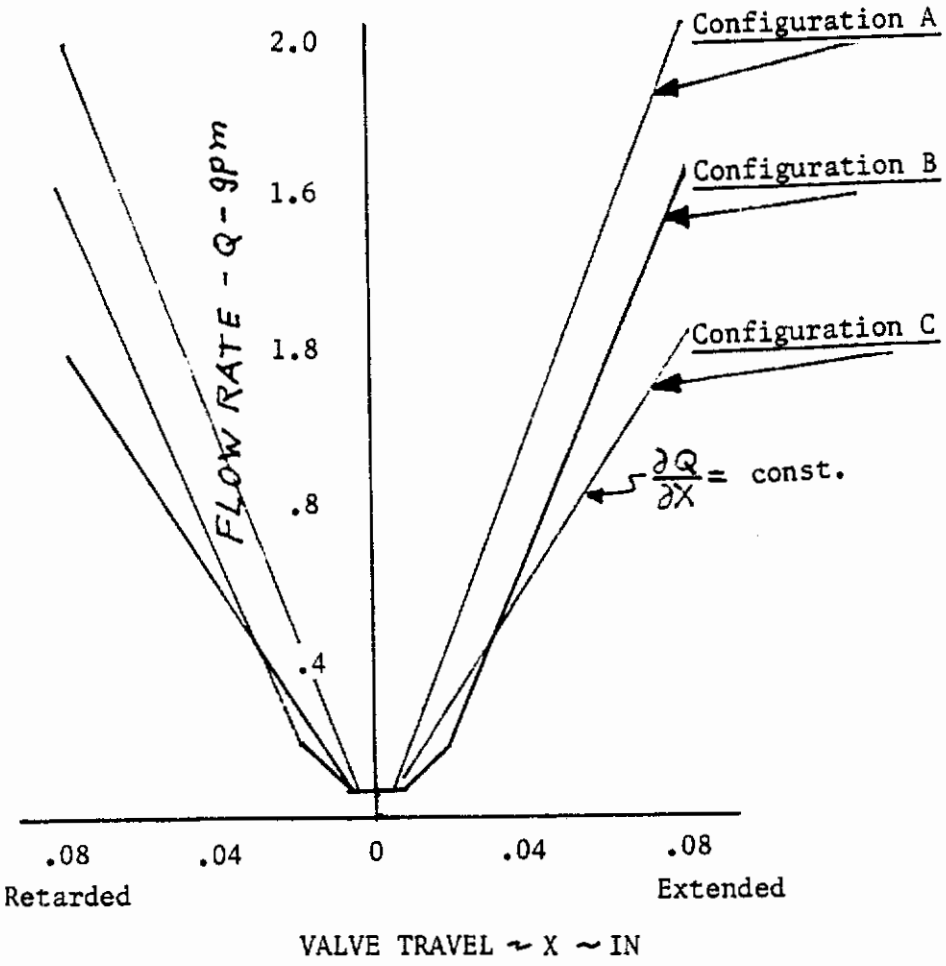

Figure 17 SERVO VALVE CHARACTERISTICS

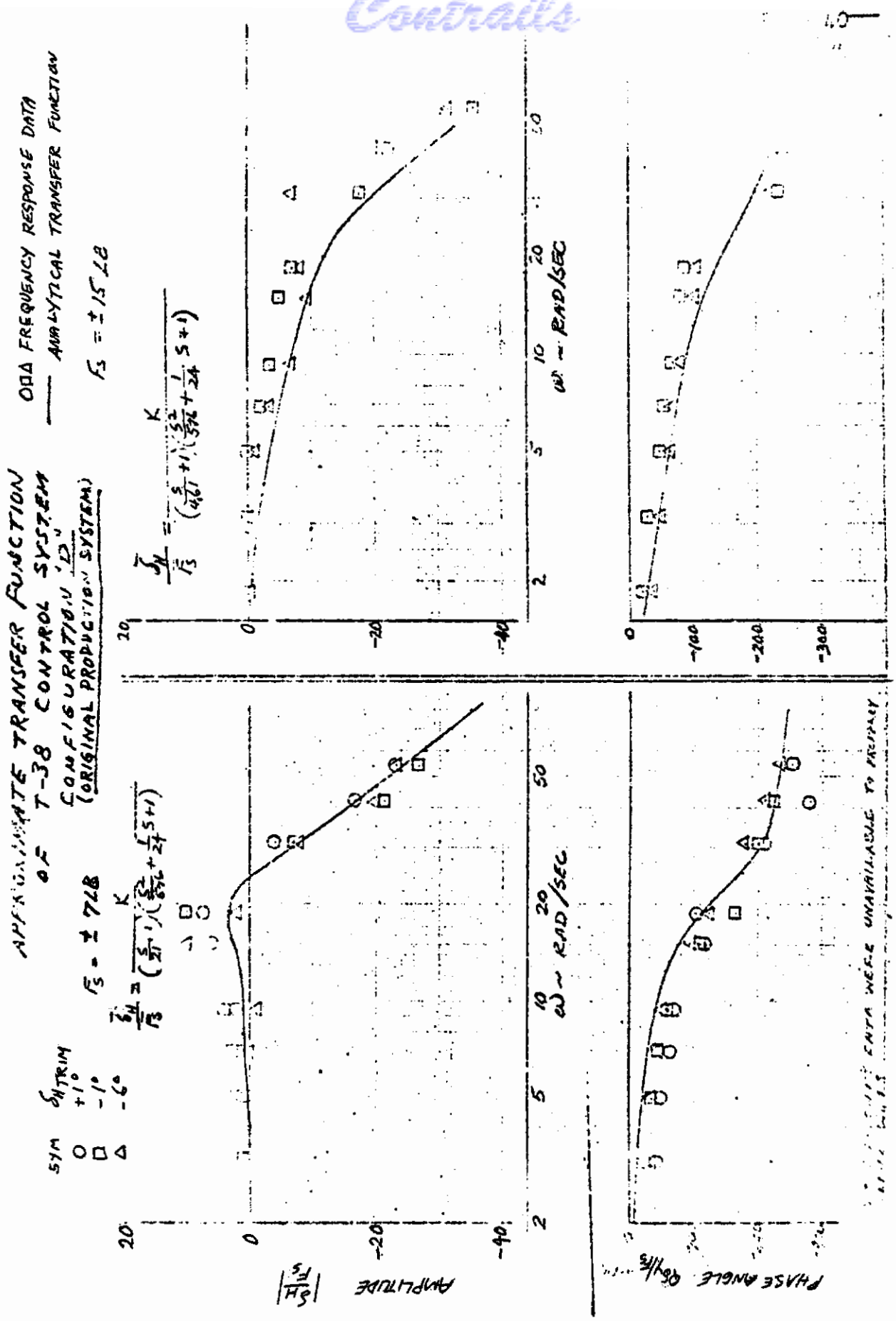

Figure 18 CONTROL SYSTEM FREQUENCY RESPONSE ~ TEST STAND

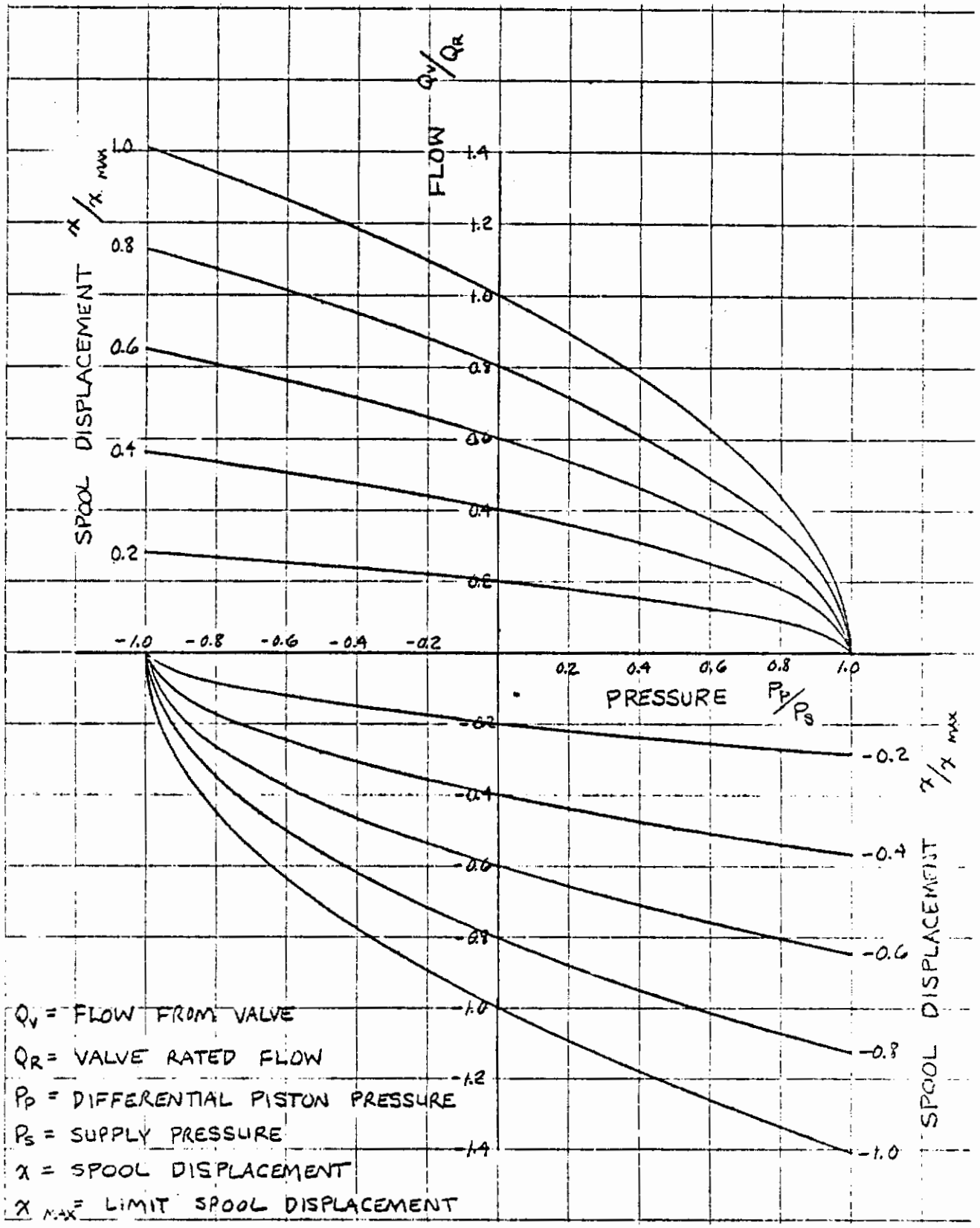

Figure 19 DIMENSIONLESS FLOW-PRESSURE CHARACTERISTICS OF A CLOSED-CENTER, 4-WAY VALVE

Ralph Smith, SRL: Smith pointed out that the phase angle between two time signals can be measured as the distance from the positive peak of one to the next positive peak of the other. He noted further that Chalk had determined the phase between F_s and θ by measuring from the peak of F_s in the pull direction to the peak of θ in the nose-up direction and obtained 255°. Chalk's claim is that this value differs by nearly 180° from that obtained by direct estimation from the STI transfer function. Smith pointed out that Chalk's measurement and subsequent analyses are in error and that the STI results are correct. The error, he claimed, is due to the static gain convention used by STI in the transfer function. Specifically, a push stick force F_s is positive, not a pull force. The fact that a pull stick force yields a nose-up attitude change, is true but irrelevant since the transfer function is predicated on the convention that push F_s is the positive sense. This change of sign accounts for what Chalk claimed is a 180° phase error. It should be noted for the record that the θ / F_s transfer function used by Chalk (p. 14 of his paper) has the wrong sign of the static gain. Since this is proportional to $M_{\delta e}$, and since $M_{\delta e}$ is less than zero in the convention used by STI, then a minus sign should precede the static gain of 0.0084. This same error appears in Smith PIO report (FDL-TR-77-57) where it was, in fact, a typographical omission. When the θ to F_s phase is measured from the T-38 PIO time history as the angle between the peak of F_s in the pull direction and the maximum nose-down θ, then there is no inconsistency between the time traces and the STI time traces. This, Smith claims, is the proper measurement technique.

Chick Chalk, Calspan: [Mr. Chalk expressed disagreement.] I took great care in interpreting sign conventions, trace recording senses on the PIO record and signs of numbers in transfer functions. In drawing the phase diagrams in Figure 11, I chose to relate "pull" force, "nose up" attitude and "trailing edge up" stabilizer. The "pull" force peak is used as the reference. The plus sign on the low frequency gain constant in the θ/F_s transfer function in Table 1 (t.0084) did not result from a typographical error or accident.

I chose to define "pull" force and "nose-up" pitch as positive which is consistent with the convention I used in the phase diagram. In calculating the phase between stabilizer and pitch attitude, θ/δ_H, I defined δ_H "trailing edge up" as positive. Thus pitch attitude "lags" trailing edge up stabilizer by 128° at ω=7.4 rad/sec. In evaluating the transfer function for stabilizer to stick force that is indicated on Figure 11 of my paper, I again used "pull" force and "trailing edge up" stabilizer as references. Thus at low frequency the stabilizer moves "in phase" with the stick force. At ω=7.4 rad/sec the stabilizer will "lead" stick force by 46.7° according to the analytical model but it "lags" stick force by 127° according to the empirical model at the top of Fig 11.

I hope this discussion clarified the situation.